BIOMOLECULES & THERAPEUTICS

Original Article
Biomol Ther 25(5), 535-544 (2017)

Inhibitory Effect of Carnosol on Phthalic Anhydride-Induced Atopic Dermatitis via Inhibition of STAT3

Do Yeon Lee[1], Chul Ju Hwang[1], Ji Yeon Choi[1], Mi Hee Park[1], Min Ji Song[1], Ki Wan Oh[1], Dong Ju Son[1], Seung Hwa Lee[2], Sang Bae Han[1] and Jin Tae Hong[1,*]

[1]College of Pharmacy and Medical Research Center,
[2]Department of Industrial Cosmetics, Chungbuk National University, Cheongju 28160, Republic of Korea

Abstract

Carnosol is a phenolic antioxidant present in rosemary (*Rosmarinus officinalis*). It is known for anti-inflammatory effects, analgesic activity and anti-cancer effects. However, no study has been dedicated yet to its effect on atopic dermatitis (AD). Here, we show that carnosol effectively inhibited LPS-induced nitric oxide (NO) generation and expression of inflammatory marker proteins (iNOS and COX-2) in RAW 264.7 cells. In addition, carnosol effectively inhibits the phosphorylation of STAT3 and DNA binding activity in RAW 264.7 cells. Pull down assay and docking model analysis showed that carnosol directly binds to the DNA binding domain (DBD) of STAT3. We next examined the anti-atopic activity of carnosol (0.05 $\mu g/cm^2$) using 5% Phthalic anhydride (PA)-induced AD model in HR1 mice. Carnosol treatment significantly reduced 5% PA-induced AD like skin inflammation in skin tissues compared with control mice. Moreover, carnosol treatment inhibits the expression of iNOS and COX-2 in skin tissue. In addition, the levels of TNF-α, IL-1β, and Immunoglobulin-E in blood serum was significantly decreased in carnosol treated mice compared with those of 5% PA treated group. Furthermore, the activation of STAT3 in skin tissue was decreased in carnosol treated mice compared with control mice. In conclusion, these findings suggest that carnosol exhibited a potential anti-AD activity by inhibiting pro-inflammatory mediators through suppression of STAT3 activation via direct binding to DBD of STAT3.

Key Words: Atopic dermatitis, STAT3, Carnosol

INTRODUCTION

Atopic dermatitis (AD) is a chronic inflammatory skin disease and commonly occurs during infancy or childhood but can also occur in adults. AD is characterized by chronic eczematous and pruritic skin lesions, which are caused by infiltration of inflammatory cells such as mast cells, eosinophils, monocytes/macrophages and T lymphocytes (Lim *et al*., 2016). Mast cells are key mediators of immediate allergic responses and anaphylaxis, releasing histamine and other inflammatory mediators of inflammation (Siegel *et al*., 2013). The developmental trigger in most patients is elevated levels of serum immunoglobulin E (IgE) and circulating eosinophils due to increased production of interleukin (IL)-4, IL-5 and IL-13 by Th2 cells. The pro-inflammatory cytokines IL-1, IL-6, and TNF-α are produced by inflammatory dendritic epidermal cells which are differentiated from recruited monocytes in the acute phase of AD. Other cytokines, such as IL-4, IL-13, IL-17, interferon-γ (IFN- γ) are also increased in AD skin lesions (You *et al*., 2016).

Rosmarinus officinalis L. (family *Lamiaceae*), popularly called rosemary, is native to the Mediterranean region and is now widely spread in European countries. It has been used in folk medicine with several pharmacological effects being associated to its consumption, including its anti- inflammatory effects due to its high antioxidant and antimicrobial activities (Rocha *et al*., 2015; Oliveira Gde *et al*., 2016). As one of the main active diterpene in rosemary, carnosol (CS) has been largely investigated for anti-tumoral, anti-inflammatory and anti-oxidant activities *in vitro* and *in vivo* (Ortuno *et al*., 2015; Sanchez *et al*., 2015). In previously studies, carnosol significantly inhibited inflammatory responses such as IL-1β, tumor necrosis factor-α (TNF-α) and increased IL-10 in inflamed mice skin (Yao *et al*., 2014; Schwager *et al*., 2016). Carnosol also inhibited NO generation and expression of inducible nitric oxide synthase (iNOS), cyclooxygenase-2 (COX-2) in RAW

Open Access **https://doi.org/10.4062/biomolther.2017.006**

Received Jan 17, 2017 **Revised** Apr 19, 2017 **Accepted** May 2, 2017
Published Online Jun 27, 2017

***Corresponding Author**
E-mail: jinthong@chungbuk.ac.kr
Tel: +82-43-261-2813, Fax: +82-43-268-2732

264.7 cells and mice skin (Mengoni *et al*., 2011). The constitutive phosphorylation, the DNA binding and reporter gene activity of signal transducer and activator of transcription-3 (STAT3) was also reduced by treatment with carnosol in human colon cancer HCT116 cells (Park *et al*., 2014).

Several studies have indicated that the activation of JAK-STAT signaling occurs in the skin of AD patients, and the serum levels of STAT3 were increased in childhood AD (Lyu *et al*., 2014; Amano *et al*., 2015). STAT3 is also involved in Ig-E dependent mast cell degranulation of human and mice mast cells in AD (Siegel *et al*., 2013; Boos *et al*., 2014). It is also well known that activated STAT3 downregulates keratinocyte differentiation which is involved in skin barrier formation (Amano *et al*., 2015). Several cytokines are involved in the AD development through modification of STAT3 activation (Bao *et al*., 2012). Activation of STAT3 is increased by IL-23, IL-12 and IL-6 in T cells in the edema formation, lymphocyte infiltration, and keratinocyte proliferation of AD (Fridman *et al*., 2011). It was also reported that IL-31 level was elevated by the activation of STAT3 in AD patients (Lee *et al*., 2012). Thus, application of topical and systemic anti-inflammatory agents inhibiting STAT3 is important for the treatment of AD (He *et al*., 2017).

Several pharmacological effects such as anti-oxidant, anti-inflammatory, anti-carcinogenic activities, and neuroprotective effects of carnosol have been studied. However, no study has been dedicated yet to its potential effect on AD. Therefore, we study the anti-AD effects of carnosol *in vitro* and *in vivo*.

MATERIALS AND METHODS

Materials

Carnosol and phthalic anhydride were purchased from Sigma Aldrich (St. Louis, MO, USA).

Ethical approval

The animal study was carried out according to the guidelines for animal experiments of the Institutional Animal Care and Use Committee (IACUC) of Laboratory Animal Research Center at Chungbuk National University, Cheongju, Korea (CBNUA-929-16-01). The mice were housed three mice per cage with an automatic temperature control (21-25°C), relative humidity (45-65%), and 12 h light-dark cycle illuminating from 07:00 a.m. to 07:00 p.m. Food and water were available ad libitum. During this study, all mice were specially observed for normal body posture, ataxia, urination, etc. two times per day.

Animal treatment

The protocols for the animal experiment used in this study were carefully reviewed for ethical and scientific care procedures and approved by the Chungbuk National University-Institutional Animal Care and Use Committee (Approval Number CBNU-2015-0976). Eight week old male HR1 mice (Saeronbio, Uiwang, Korea) were maintained and handled in accordance with the humane animal care and use guidelines of Korean FDA. HR1 mice (eight-week-old, n=32) were randomly divided into one of three groups. Age-matched HR1 mice were used as the control group (control, n=8). In the first group (control, n=8), nothing was applied. In the second group (Vehicle, n=8), 200 μl of Dimethyl sulfoxide (DMSO) was spread on the dorsum of the ears and back skin three times a week for four weeks. The third group (PA, n=8), 100 μl (20 μl/cm^2) of 5% phthalic anhydride solution was applied. The fourth group (carnosol 0.05 μg/cm^2, n=8) was first applied with PA, and after three hours 100 μl (20 μl/cm^2) of 10 μM of carnosol was applied.

Evaluation of dermatitis severity

The severity of dermatitis on the ear and dorsal regions was evaluated twice per week. The development of erythema/hemorrhage, scarring/dryness, edema, and excoriation/erosion was scored as 0 (none), 1 (mild), 2 (moderate), or 3 (severe). The total clinical dermatitis severity score for each mouse was defined as the sum of the individual scores (Matsuda *et al*., 1997; Sung *et al*., 2016).

Measurement of body weight, ear thickness and lymph node weight

Alterations of body weight during the experimental procedure were measured with an electronic balance (Mettler Toledo, Greifensee, Switzerland) once a week for four weeks. Weights of lymph nodes collected from the sacrificed mice were also measured by the same method. Ear thickness was measured using a thickness gauge (Digimatic Indicator, Matusutoyo Co., Tokyo, Japan) to determine the degree of allergic skin inflammation induced by PA treatment.

Histological techniques

Ear and back skins were removed from mice, fixed with 10% formalin, embedded in paraffin wax, routinely processed, and then sectioned into 5 μm thick slices. The skin sections were then stained with hematoxylin and eosin (H&E) or toluidine blue. The thickness of the epidermis and dermis were also measured using the Leica Application Suite (Leica Microsystems, Wetzlar, Germany).

Enzyme-linked immunosorbent assay (ELISA) for detection of serum IgE concentration

The serum IgE concentration was measured using an ELISA kit (Shibayagi, Inc., Gunma, Japan) according to the manufacturer's instructions. In brief, captured antibodies were plated in the Nunc C bottom immunoplate supplied in the kit. Next, wells were washed with washing solution (50 mM Tris, 0.14 M NaCl, 0.05% Tween 20, pH 8.0) three times. Then, serum samples and standards diluted with buffer solution were added to the wells, and the plate was incubated for 2 h. The wells were washed again with washing solution, 50 μl of Biotin-conjugated anti-IgE antibodies (1000-fold dilution) were added to each well and incubated further for 2 h to bind with captured IgE. The wells were washed again with washing solution, after which horseradish peroxidase-conjugated detection antibodies (2000-fold dilution) were added to each well and incubated for 1 h. An enzyme reaction was then initiated by adding tetramethylbenzidine (TMB) substrate solution (100 mM sodium acetate buffer pH 6.0, 0.006% H_2O_2) and the plate was incubated at room temperature in the dark for 20 min. Finally, the reaction was terminated by adding acidic solution (reaction stopper, 1 M H_2SO_4), and absorbance of the yellow product was measured spectrophotometrically at 450 nm. The final concentration of IgE was calculated using the standard curve.

Cytokine assay

By the end of the study period, blood specimens were collected. Serum levels of mouse TNF-α and IL-1β were measured by enzymelinked immunosorbent assay (ELISA) kits provided by Thermo Scientific, Inc. (Rockford, IL, USA) according to the manufacture's protocol.

Luciferase activity

RAW 264.7 cells were plated in 12-well plates (1×10^5 cells/well) and transiently transfected with STAT3-Luc plasmid using a mixture of plasmid and Lipofectamine 3000 in OPTI-MEM according to manufacturer's specification (Invitrogen, Carlsbad, CA, USA) for 24 h (Kim *et al*., 2012; Kim *et al*., 2014). The transfected cells were treated with 1, 2 and 5 μM carnosol for another 24 h. Luciferase activity was measured by using a luciferase assay kit (Promega, Madison, WI, USA), and the results were read on a luminometer as described by the manufacturer's specifications (WinGlow, Bad Wildbad, Germany).

Pull down assay

Carnosol was conjugated with cyanogen bromide (CNBr)-activated Sepharose 6B (Sigma Aldrich). Briefly, carnosol (1 mg) was dissolved in 1 ml of coupling buffer (0.1 M NaHCO3 and 0.5 M NaCl, pH 6.0). The CNBr-activated Sepharose 6B was swelled and washed in 1 mM HCl on a sintered glass filter, then washed with the coupling buffer. CNBr-activated Sepharose 6B beads were added to the carnosol containing coupling buffer and incubated at 4ºC for 24 h. The carnosol conjugated with Sepharose 6B was washed with three cycles of alternating pH wash buffers (buffer 1, 0.1 M acetate and 0.5 M NaCl, pH 4.0; buffer 2, 0.1 M Tris HCl and 0.5 M NaCl, pH 8.0). Carnosol-conjugated beads were then equilibrated with a binding buffer (0.05 M Tris HCl and 0.15 M NaCl, pH 7.5). The control unconjugated CNBr-activated Sepharose 6B beads were prepared as described above in the absence of carnosol. The cell lysate or STAT3 recombinant protein (Abnova, Taipei, Taiwan) were mixed with carnosol-conjugated Sepharose 6B or Sepharose 6B at 4ºC for 24 h. The beads were then washed three times with TBST. The bound proteins were eluted with SDS loading buffer. The proteins were then resolved by SDS-PAGE followed by immunoblotting with antibodies against STAT3 (1:1000 dilution, Santa Cruz Biotechnology Inc., Santa Cruz, CA, USA).

Western blot analysis

100 mg of mice skin tissues or about 1×10^6 cells were harvested and homogenized with lysis buffer [50 mM Tris pH 8.0, 150 mM NaCl, 0.02% sodium azide, 0.2% SDS, 1 mM phenyl methylsulfonyl fluoride (PMSF), 10 μl/ml aprotinin, 1% igapel 630 (Sigma Aldrich), 10 mM NaF, 0.5 mM EDTA, 0.1 mM EGTA and 0.5% sodium deoxycholate]. The extracts were centrifuged at 23,000 g for 1 h. Equal amounts of protein (20 μg) was separated on a sodium dodecyl sulfate (SDS)/10%-polyacrylamide gel, and then transferred to a nitrocellulose membrane (Hybond ECL, Amersham Pharmacia Biotech Inc., Piscataway, NJ, USA). Blots were blocked for 2 h at room temperature with 5% (w/v) non-fat dried milk in Tris-buffered saline [10 mM Tris (pH 8.0) and 150 mM NaCl] solution containing 0.05% tween-20. The membrane was incubated for 4 h at room temperature with specific antibodies: rabbit polyclonal antibodies against iNOS and COX-2 (1:500) (Santa Cruz Biotechnology Inc.), and mouse polyclonal antibodies against STAT3 (1:500) (Santa Cruz Biotechnology Inc.) were used in this study. The blot was then incubated with the corresponding conjugated anti-rabbit immunoglobulin G-horseradish peroxidase (Santa Cruz Biotechnology Inc.). Immunoreactive proteins were detected with the enhanced chemiluminoscent (ECL) western blotting detection system.

Cell culture

The RAW 264.7 murine macrophage cell line was obtained from the Korea Cell Line Bank (Seoul, Korea). These cells were grown at 37°C in DMEM medium supplemented with 10% FBS, penicillin (100 units/ml) and streptomycin sulfate (100 μg/mL) in a humidified atmosphere of 5% CO_2. Cells were incubated with carnosol at various concentrations (1, 2, or 5 μM) or positive chemicals and then stimulated with LPS 1 μg/mL for the indicated time in figure legends. Various concentrations of carnosol dissolved in ethanol were added together with LPS. The final concentration of ethanol used was less than 0.05%. Cells were treated with 0.05% ethanol as the vehicle control.

Electro mobility shift assay

EMSA was performed according to the manufacturer's recommendations (Promega). Briefly, astrocytes were washed twice with 1×PBS, followed by the addition of 1 ml of PBS, and the cells were scraped into a cold Eppendorf tube. Cells were spun down at 15,000 rpm for 5 min, and the resulting supernatant was removed. Solution A (50 mM HEPES, pH 7.4, 10 mM KCl, 1 Mm EDTA, 1 mM EGTA, 1 mM dithiothreitol, 0.1 μg/ml PMSF, 1 μg/ml pepstatin A, 1 μg/ ml leupeptin, 10 μg/ml soybean trypsin inhibitor, 10 μg/ml aprotinin, and 0.5% Nonidet P-40) was added to the pellet in a 2:1 ratio (v/v) and incubated on ice for 10 min. Solution C (solution Aþ 10% glycerol and 400 mM KCl) was added to the pellet in a 2:1 ratio (v/v) and vortexed on ice for 20 min. The cells were centrifuged at 15,000 g for seven minutes, and the resulting nuclear extract supernatant was collected in a chilled Eppendorf tube. The proteins of mice brains were extracted as the method in astrocytes. STAT3 (5'-GAT CCT TCT GGG AAT TCC TAG ATC-3', Santa Cruz Biotechnology) were end labeled using T4 polynucleotide kinase and (γ-32P) ATP for 10 min at 37ºC. Gel shift reactions were assembled and allowed to incubate at room temperature for 10 min followed by the addition of 1 μl (50,000 to 200,000 cpm) of ^{32}P-labeled oligonucleotide and another 20 min of incubation at room temperature. Subsequently, 1 μl of gel loading buffer was added to each reaction and loaded onto a 4% nondenaturing gel and electrophoresed until the dye was 75% of the way down the gel. The gel was dried at 80ºC for 2 h and exposed to film overnight at -70ºC. The relative density of the protein bands was scanned by densitometry using MyImage (SLB, Seoul, Korea), and quantified by Labworks 4.0 software (UVP Inc., Upland, CA, USA).

Nitrite quantification assay

The NO was determined through the indication of nitrite level in the cell culture media. The nitrite accumulation in the supernatant was assessed by Griess reaction (Szczepanik and Ringheim, 2003). The RAW 264.7 murine macrophages were seeded into 6-well plates (1×10^6 cells/well) with 2 ml of cell culture media and incubated for 24 h. This was followed by discarding the old culture media and replacing them with new

media to maintain the cells. Different concentrations of carnosol (1, 2, and 5 μM) were pretreated with the RAW 264.7 macrophages. Induction of RAW 264.7 macrophages with LPS (1 μg/mL) for all samples were conducted except in the control group for another 24 h. Then, 100 μl of the collected supernatants was added with 100 μl of Griess reagent (0.1% NED, 1% sulphanilamide, and 2.5% phosphoric acid) and incubated in room temperature for 10 min in the dark. The absorbance was determined by using a microplate reader at 540 nm wavelength. The NO concentration was determined by comparison to the standard curve.

Statistical analysis

The experiments were conducted in triplicate, and all experiments were repeated at least three times with similar results. The data were expressed as the means ± SEM. Statistical analysis was done using the one-way ANOVA test, with the following significance levels: *p<0.05, $^{\#}p$<0.05.

RESULTS

Interaction between carnosol and STAT3

The chemical structure of carnosol is shown in Fig. 1A. We performed a pull-down assay and molecular docking experi-

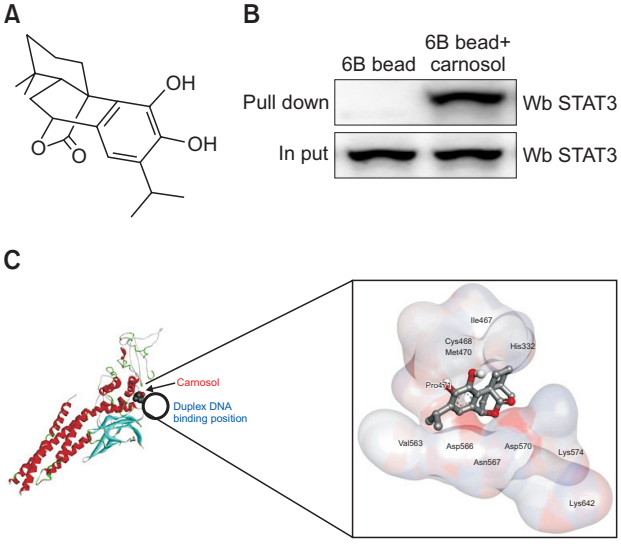

Fig. 1. Chemical structure of carnosol (A). The docking model of carnosol with STAT3 is as described in the Materials and Methods section. Pull-down assay identifies an interaction between the carnosol and STAT3. carnosol was conjugated with carnosol-activated Sepharose 6B (B). Structural interaction between carnosol and STAT3 (C).

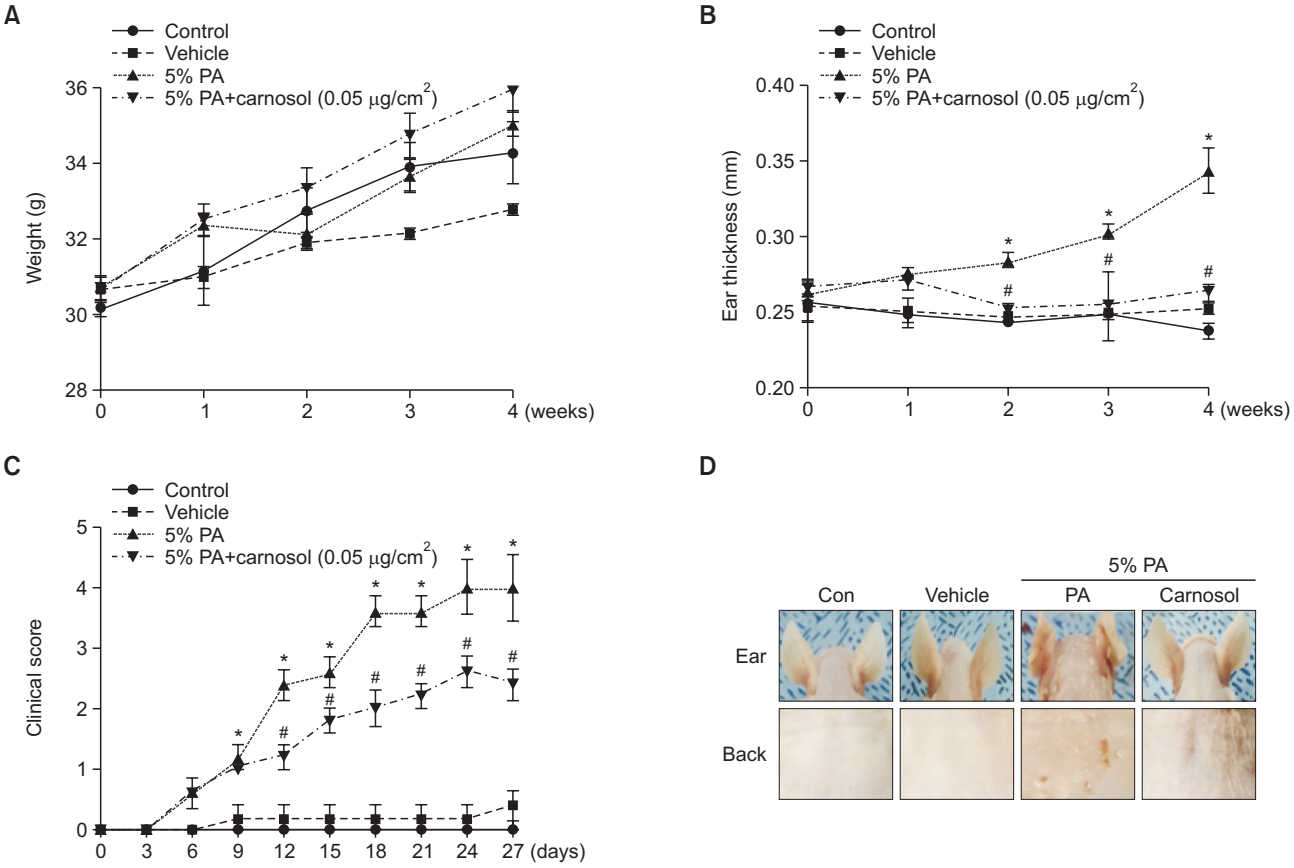

Fig. 2. Differences in body weight, ear thickness, ear phenotypes and back phenotypes. Body weights of mice in the four groups were measured with a chemical balance (A). PA solution was repeatedly applied to the dorsum of ear and back during topical application of carnosol. After 4 weeks, ear thickness (B), clinical score (C) and clinical features (D) were observed by following the procedure described in Materials and Methods. *p<0.05, $^{\#}p$<0.05.

ment between carnosol and STAT3 using carnosol-sepharose 6B beads. The binding of carnosol to STAT3 was then detected by immunoblotting with an STAT3 antibody. The results indicated that carnosol interacted with cell lysates containing STAT3 from RAW 264.7 cells as well as recombinant STAT3 protein (Fig. 1B). To further identify the binding of STAT3 to carnosol, we performed computational docking experiments with carnosol and STAT3. The binding study was performed using Autodock Vina software and showed that carnosol binded to STAT3 (carnosol binds to: His332, Ile467, Cys468, Met470, Pro471, Val563, Asp566, Asn567, Asp570, Lys574, and Lys642) (Fig. 1C).

Effects of carnosol treatment on ear thickness and morphology

To determine whether or not treatment with carnosol can suppress the changes in ear phenotype induced by PA treatment, clinical score, ear thickness and morphology of ear were observed. Ear thickness significantly increased in PA treated mice compared to the control and vehicle treated group. On the other hand, ear thickness in the carnosol treated group was decreased (Fig. 2B). Clinical score of AD increased rapidly in PA induced mice. The dermatitis severity score was significantly lower in mice treated with carnosol as control and vehicle treated mice. The total clinical dermatitis severity score of PA group was increased up to 4 on day 27 compared with the control or vehicle treated group. And, the score of the carnosol group was up to 2.4 on day 27 (Fig. 2C). Furthermore, symptoms consisting of erythma, dry skin, edema, excoriation and erosion were observed in the PA treated group compared with the control or vehicle treated group. Changes in body weight and ear thickness were measured during the experimental period. No significant difference in body weight was detected after any of the treatments (Fig. 2A). However, ear and back morphology of 5% PA treatment group were dramatically reversed upon carnosol treatment (Fig. 2D).

Effect of carnosol treatment on lymph node weight and IgE concentration

The lymph node size and weight are significantly increased in the AD condition (Fig. 3A, 3B). We thus determined whether or not carnosol could suppress the increases in lymph node weight and IgE concentration. We evaluated the auricular lymph node weight and serum IgE concentration. PA treatment induced an increase in lymph node weight compared with the control or vehicle treated mice. However, the weight of lymph node was significantly reduced in the carnosol treated mice (Fig. 3B). It is well known that hyperproduction of Ig-E is characteristic features of allergic hypersensitivity as well as an indicator of the magnitude of the allergic immune response including AD (Suzuki *et al*., 2016). The serum Ig-E concentration was measured in all mice groups to determine whether carnosol inhibits the allergic response induced by PA. Topical application of PA induced a significant increase in serum Ig-E concentration compared with control (369.0 ± 43.56). However, the level was significantly decreased by the treatment of carnosol (114.5 ± 6.696) (Fig. 3C). Furthermore, topical application of PA induced a significant increase in neutrophils of whole blood (62.44 ± 2.315). However, the level was significantly decreased by the treatment of carnosol (33.58 ± 1.548) (Fig. 3D).

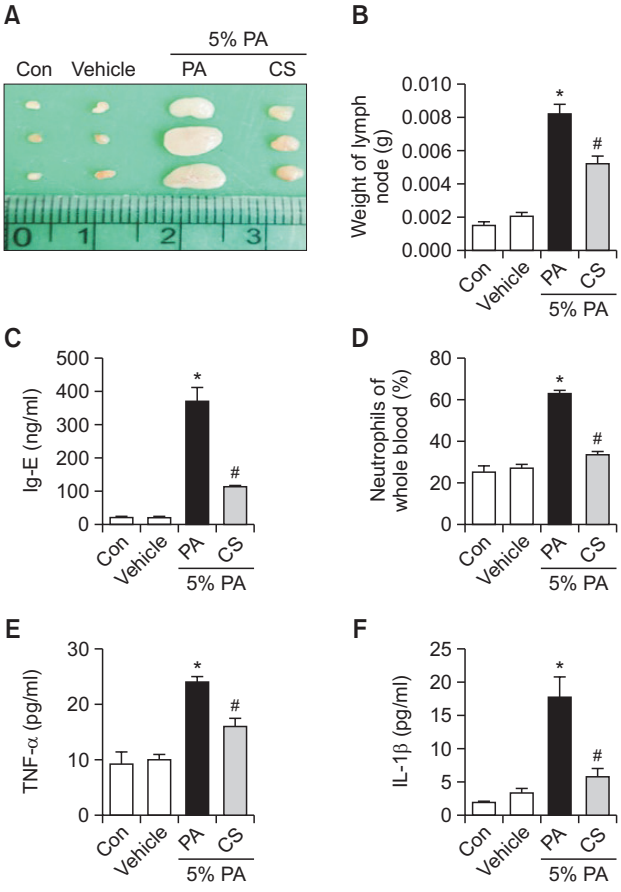

Fig. 3. Changes in auricular lymph node weight, and serum cytokine concentration. The auricular lymph nodes were harvested from the neck regions of the mice using a microscissor, after which they were taken picture (A) and weighed (B). Serum used to measure the cytokine concentration was prepared from blood samples collected from the abdominal veins of mice. Serum IgE (C), TNF-α (D) and IL-1β (E) concentration were quantified by ELISA. Whole blood used to measure the neutrophils (F). Data shown are the mean ± SEM (n=8). $^{*}p<0.05$, $^{\#}p<0.05$.

Effect of carnosol on the release of inflammatory cytokines

To determine if carnosol treatment could induce alterations in the inflammatory cytokines in PA-induced skin inflammation, the level of TNF-α and IL-1β was measured in the mouse serum of the control, vehicle, PA and PA+ carnosol treated group. The level of TNF-α and IL-1β were generally higher in the PA treated group than the control or vehicle treated group. However, these levels in the carnosol treated group were significantly decreased to the level of the control or vehicle treated group (Fig. 3E, 3F).

Effect of carnosol treatment on ear and back histology

To investigate the inhibitory effect of carnosol treatment on ear and back histology, histological analysis of the ear and back skin was performed. The hematoxylin and eosin stained ear and back tissues showed the epidermis and dermis were thicker in the PA treated group than in the control or vehicle treated group. Also, the ear and back skin showed inflammatory cell infiltration of the dermis in PA-induced mice. However, the thickness and inflammatory cell infiltration were sig-

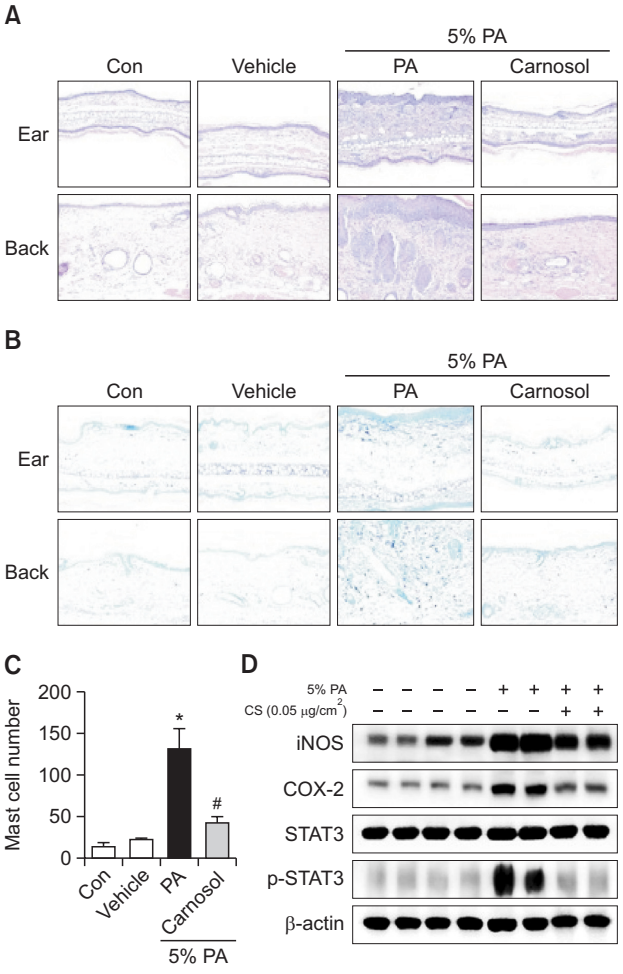

Fig. 4. Ear and back histology and protein expressions of iNOS and COX-2 and inhibitions of STAT3 (phosphorylation) by topical application of carnosol in back skin. Tissues were excised, fixed in 10% formaldehyde, embedded in paraffin, and sectioned. Representative photographs of ear skin sections stained with hematoxylin and eosin or toluidine blue (original magnification X200) (A and B). Mast cell numbers (C). Mast cells in toluidine blue-stained sections were counted under a microscope (X200). Data shown are the mean ± SEM (n=8). Alteration of the expression of iNOS and COX-2 proteins were measured by Western blotting (A). Equal amounts of nuclear proteins (20 μg/lane) or total proteins (20 μg/lane) were subjected to 8% SDS-PAGE, and expression of STAT3 and p-STAT3 protein were detected by Western blotting using specific antibodies. β-actin protein were used here as an internal control (D). Data shown are the mean ± SEM (n=8). *p<0.05, $^{\#}p$<0.05.

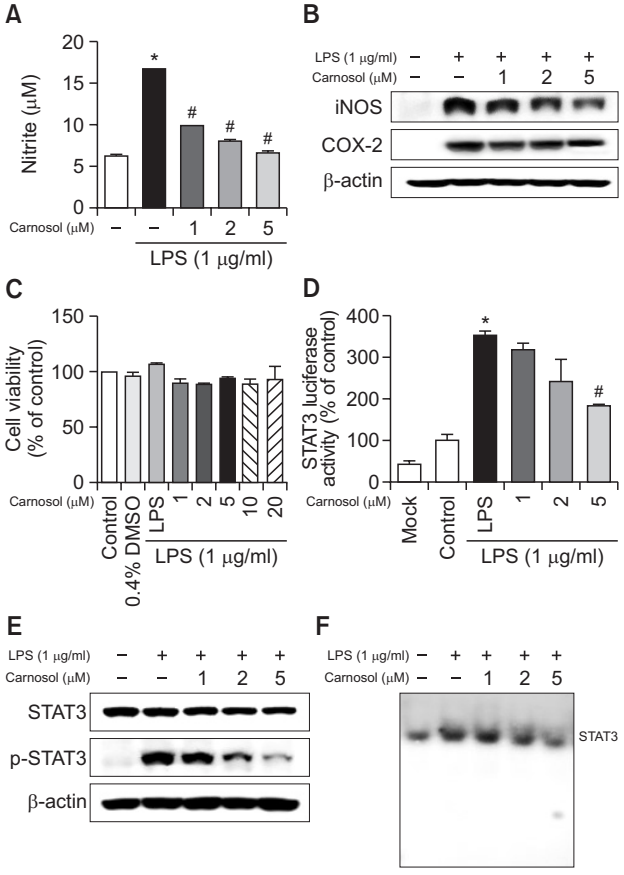

Fig. 5. Effect of carnosol on LPS-induced NO release and on protein expressions of iNOS and COX-2 in RAW 264.7 cells. NO level was determined by Griess reaction as described in Methods, in supernatants from RAW 264.7 cells (A). Cells were treated with 1 μg/ml of LPS alone, or with LPS plus different concentrations (1, 2, 5 μM) of carnosol, at 37°C for 24 h. Equal amounts of total protein (20 μg/lane) were subjected to 8% SDS-PAGE, and the expression of iNOS, COX-2, STAT3 and p-STAT3 were detected by Western blotting using specific antibodies in RAW 264.7 cells (B and E). β-actin protein was used here as an internal control. Similar results were obtained from at least three different sets of experiment. Cell viability was evaluated using a MTT assay as described in Methods. RAW 264.7 cells (C). RAW 264.7 cells were transfected with a p-STAT3-Luc plasmid (5×STAT3), and then treated with LPS (1 μg/ml) either alone or with KRICT NO.9 (1, 2, 5 μM) for 37°C for 24 h. Luciferase activity was then determined as described in Methods (D). The activation of STAT3 was investigated using EMSA (F). Values represent means ± SD for three independent experiments performed in triplicate. *p<0.05. $^{\#}$ indicates significantly different from LPS treated group (p<0.05).

nificantly decreased in the carnosol treated group (Fig. 4A). The ear and back tissues were stained with toluidine blue to determine PA-induced mast cell infiltration to the dermis (Fig. 4B). The number of mast cells in the dermis of back skin increased significantly in PA-induced mice (131.3 ± 25.12) compared with control mice (13.00 ± 5.508), and this increase was reduced with a topical application of carnosol (Fig. 4C).

Effect of caronosol on expression of iNOS and COX-2, and p-STAT3 in PA induced AD mice skin

To investigate whether the inhibitory effect of carnosol on expression of p-STAT3 in PA-induced AD model exists, the back skin tissues were prepared and assayed by western blot. The back skin of PA treated mice showed significant phosphorylation of STAT3 when compared to the control group. In contrast, carnosol significantly inhibited phosphorylation of STAT3. However, there was no difference in STAT3 (Fig. 4D). In addition, protein expressions of iNOS and COX-2 were significantly increased in PA-treated AD mice, but significantly decreased with carnosol treatment (Fig. 4D).

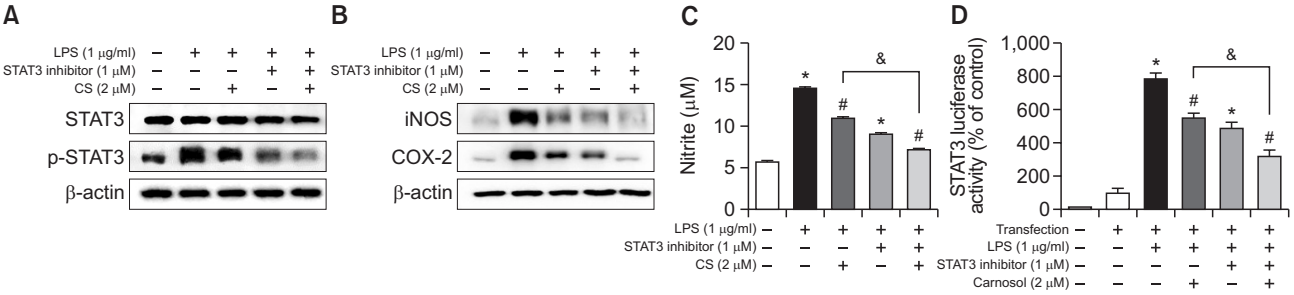

Fig. 6. Involvement of STAT3 in the inhibitory effect of carnosol on the LPS-induced STAT3, NO generation and expression of iNOS and COX-2 in RAW 264.7 cells. RAW 264.7 cells were cultured with STAT3 inhibitor (1 μM) and carnosol (2 μM) at 37°C for 15 min and 24 h. Equal amounts of total proteins (20 μg/lane) were subjected to 8% SDS-PAGE, and activation of STAT3 (phosphorylation), the expression of iNOS and COX-2 was detected by Western blotting using specific antibodies in RAW 264.7 cells (A and B).The level of NO generation was determined by NO assay (C). RAW 264.7 cells were transfected with a p-STAT3-Luc plasmid (5×STAT3), and then treated with LPS (1 μg/ml) either alone or with STAT3 inhibitor (1 μM) and carnosol (2 μM) for 37°C for 24h. Luciferase activity was then determined as described in Methods (D). Similar results were obtained from at least three different sets of experiment. Values are presented as mean ± SD for three independent experiments performed in triplicate. *p<0.05 compared to control, $^{\#}p$<0.05 compared LPS. $^{\&}p$<0.05 compared treated with LPS alone and treated with STAT3 inhibitor.

Effect of carnosol on LPS-induced NO production and iNOS and COX-2 expression in RAW 264.7 cells

Inflammation is a critical factor in AD, and NO is an indicator of inflammation in the skin (Tsunekawa *et al*., 2017). Thus, the effect of carnosol on LPS-induced NO production in RAW 264.7 cells was investigated by measuring the released nitrite in the culture medium by Griess reaction. Treatment of LPS (1 μg/mL) significantly increased NO level in RAW 264.7 cells. After co-treatment with LPS and carnosol (1, 2, 5 μM) for 24 hours, LPS-induced NO level was decreased remarkably in a concentration dependent manner (Fig. 5A). In addition, to determine whether carnosol inhibits the NO production via inhibition of inflammatory gene expression, we determined iNOS and COX-2 expression by Western blot analysis. As shown in Figure 1A, iNOS and COX-2 protein expression was significantly increased in response to LPS (1 μg/mL) after 24 hours. Co-treatment with carnosol (1, 2, 5 μM) caused decrease of LPS-induced iNOS and COX-2 expression in RAW 264.7 cells in a concentration dependently (Fig. 5B). However, the doses of carnosol tested did not have any toxic effects (Fig. 5C)

Effect of carnosol on STAT3 activities

STAT3 regulates inflammation through the regulation of several genes. To investigate whether carnosol is able to attenuate LPS-induced STAT3 transcriptional activity, we used RAW 264.7 cells transiently transfected with STAT3-Luc plasmid for luciferase activity measurement. Cells were then treated with LPS (1 μg/mL) or co-treated with LPS and carnosol for 24 h. Treatment with carnosol resulted in a concentration-dependent suppression of luciferase activity induced by LPS (Fig. 5D). To investigate whether carnosol can prevent LPS-induced STAT3 activity, RAW 264.7 cells were treated with LPS (1 μg/ml) or co-treated with LPS and carnosol (1, 2 and 5 μM) for 15 min. LPS significantly induced STAT3 phosphorylation, but LPS-induced STAT3 phosphorylation was markedly inhibited by co-treatment with carnosol in RAW 264.7 cells in a concentration dependent manner (Fig. 5E). Consistent with the inhibitory effect on STAT3 phosphorylation, DNA binding activity of STAT3 elevated by LPS was significantly reduced by carnosol in RAW 264.7 cells (Fig. 5F).

Involvement of the STAT3 pathway in the inhibitory effect of carnosol on LPS-induced inflammation

To further investigate the involvement of STAT3 pathway in carnosol induced anti- inflammation effects, we employed specific STAT3 inhibitor with treatment of carnosol. We determined STAT3, p-STAT3 as well as NO release after co-treatment of specific STAT3 inhibitor (stattic) with carnosol. The combination of carnosol (2 μM) and STAT3 inhibitor (static, 1 μM) significantly inhibited STAT3 phosphorylation compared to carnosol and STAT3 inhibitor (stattic) treatment alone (Fig. 6A). In addition, expression of iNOS and COX-2 significantly decreased with a combination of carnosol and STAT3 inhibitor (Fig. 6B). Treatment of carnosol (2 μM) decreased the NO generation (24.62% inhibition) and STAT3 luciferase activity (28.83%) in RAW 264.7 cells. However, the inhibitory effect of carnosol on NO generation (50.61%) and luciferase activity (58.52%) was augmented by co-treatment of carnosol with a specific STAT3 inhibitor (stattic) in RAW 264.7 cells (Fig. 6C, 6D).

DISCUSSION

AD is a chronic, relapsing, and highly pruritic inflammatory skin disease (Riis *et al*., 2016). Generally, the skin tissues of AD show hyperkeratosis, spongiosis, parakeratosis, epidermal hyperplasia, acanthosis and accumulation of lymphocytes and mast cells (Lee *et al*., 2014). Pro-inflammatory cytokines are known to induce mast cells to produce inflammatory mediators such as histamine, proteases, and chemotactic factors. Production of pro-inflammatory cytokines from mast cells and increase of neutrophils are markers of allergic inflammation (Sae-Wong *et al*., 2016; Lee *et al*., 2017). IgE-dependent mast cell activation is known to release a variety of allergic mediators, including TNF-α and histamine (Lee *et al*., 2017). In AD, dermal infiltration, mast cells, IgE and cytokines were significantly increased (Sung *et al*., 2013; Lee *et al*., 2014). Therefore, lower levels of Ig-E, cytokines, neutropils and inactivation of mast cells are important for the treatment of AD. Our data show that thickness of epidermis, Ig-E concentration, neutrophils, mast cells, cytokines involved in inflammatory

responses were significantly decreased in carnosol treated mice. These data indicate that carnosol has anti-dermatitis effects.

Several studies indicated that AD is characterized by an increased serum Ig-E level and cytokine expression (Choi *et al*., 2016). In other previous studies, a variety of anti-inflammatory compounds, such as *Aquaphilus dolomiae* extract, bee venom and fullerene C60 have showed efficacy to hinder anti-AD through decreased cytokines and Ig-E level (Aries *et al*., 2016; Shershakova *et al*., 2016; You *et al*., 2016). Our study demonstrated that carnosol treatment significantly reduced Ig-E and cytokines in PA induced mice. A number of studies have shown that nitiric oxide (NO), iNOS, and COX-2 play key roles in inflammation *in vitro* and *in vivo*. NO production by macrophages can damage cells and tissues and COX-2 appears to cause prostaglandin formation in inflammation. LPS stimulation can activate target genes encoding pro-inflammatory cytokines, chemokines, and inducible enzymes such as iNOS and COX-2 (Stempelj *et al*., 2007; Kang *et al*., 2012). In this study, carnosol reduced PA-induced expression of iNOS, COX-2 in the mice. Also, carnosol showed decreased LPS-induced expression of iNOS, COX-2 and NO production in RAW 264.7 cells. In AD, NO, iNOS and COX-2 stimulated by TNF-α/IFN-γ and IL-1β contributed to induce AD (Orita *et al*., 2011; Ahn *et al*., 2016). Some studies such as Hataedock, Quercetin, Resveratrol and K112PC-5 show that anti-AD effects via inhibition of NO production, iNOS, COX-2 and cytokines (Kang *et al*., 2008; Karuppagounder *et al*., 2014, 2015; Cha *et al*., 2016). Our study indicated that carnosol has anti-AD effect through reducing inflammatory responses.

The STATs pathway has been shown to play an essential role in the downregulation of inflammatory responses in AD (Bao *et al*., 2013; Chang *et al*., 2016). Activation of STAT3 resulted in increased release of TNF-α, IL-10, IL-1β (Zhang *et al*., 2015; Drennan *et al*., 2016). Also, activation of STAT3 was ultimately responsible for increased expression of iNOS and COX-2 (Tyagi *et al*., 2012). STAT3 is overexpressed and activated in inflammatory skin, and transgenic expression of constitutively active STAT3 in epidermal keratinocytes induced skin inflammation in mice, suggesting an important role for epidermal STAT3 signaling in inflammatory skin disease (Kumari *et al*., 2013). LPS-induced production of inflammatory cytokines was completely blocked by STAT3-deficient macrophages (Takeda *et al*., 1999). STAT3 mutation and lower monocyte chemoattractant were found in increased production of TNF-α in adult patients with hyper-IgE syndrome involved in AD (Holland *et al*., 2007). Previous studies indicated that AD is inhibited by decreased cytokines such as TNF-α, IL-1β, IL-10, IL-4 and IL-6 after topical therapy (Choi *et al*., 2016; Koppes *et al*., 2016). In this study, TNF-α and IL-1β were decreased by carnosol treatment in PA-induced mice via inhibition of STAT3 activation. We found that carnosol has a significant STAT3 binding affinity (-7.7 kcal/mol) demonstrated by the docking model and pull down assay. These data were further supported by the significant inhibitory effects of carnosol on STAT3 activity in LPS-induced RAW 264.7 cells and PA-induced mice. It is well known that STAT3 can be transcriptionally activated by phosphorylation of its two important phosphorylation sites, tyrosine 705 (in the SH2 domain) or serine 727 (in TA domain) residue. Moreover, phosphorylation leads to dimerization of STAT3 via intermolecular phosphorylated-Tyr-SH2 interactions. Therefore, it is difficult to explain how binding of carnosol to the STAT3 DBD results in inhibition of STAT3 phosphorylation with our current experimental results. One possibility is that carnosol could inhibit STAT3 phosphorylation through decreasing the p-ERK expression via suppression of STAT3 DNA-binding activity. Also, we evaluated the effect of carnosol on ERK phosphorylation which is known as upstream of STAT3 phosphorylation. Since we found that carnosol suppresses ERK activity (data not shown), the possible mechanism of STAT3 phosphorylation could be associated with ERK pathway. Similar to our data, silibinin and tricin 4'-O-(threo-β-guaiacylglyceryl) inhibit expression of iNOS, COX-2 and NO generation via inhibition of STAT3 activation (Tyagi *et al*., 2012). In addition, carnosol has synergic effects with STAT3 inhibitor via inhibition of STAT3 transcription activating and this inhibitory effect resulted in the reduction of iNOS and COX-2 expression and NO generation. These data indicate that the anti-AD effect of carnosol could be associated with an inhibitory effect on STAT3 activity. Thus, it is promising that carnosol could be a candidate compound to be developed as an anti-AD agent.

CONFLICT OF INTEREST

The authors declare no competing financial interests.

ACKNOWLEDGMENTS

This work was financially supported by the Research Year of Chungbuk National University in 2016 and supported by the National Research Foundation of Korea (NRF, and MSIP) (no. MRC 2008-0062275).

REFERENCES

Ahn, S., Siddiqi, M. H., Aceituno, V. C., Simu, S. Y., Zhang, J., Perez, Z. E., Kim, Y. J. and Yang, D. C. (2016) Ginsenoside Rg5:Rk1 attenuates TNF-α/IFN-γ-induced production of thymus- and activation-regulated chemokine (TARC/CCL17) and LPS-induced NO production via downregulation of NF-κB/p38 MAPK/STAT1 signaling in human keratinocytes and macrophages. *In vitro Cell. Dev. Biol. Anim.* **52**, 287-295.

Amano, W., Nakajima, S., Kunugi, H., Numata, Y., Kitoh, A., Egawa, G., Dainichi, T., Honda, T., Otsuka, A., Kimoto, Y., Yamamoto, Y., Tanimoto, A., Matsushita, M., Miyachi, Y. and Kabashima, K. (2015) The Janus kinase inhibitor JTE-052 improves skin barrier function through suppressing signal transducer and activator of transcription 3 signaling. *J. Allergy Clin. Immunol.* **136**, 667-677.e7.

Aries, M. F., Hernandez-Pigeon, H., Vaissiere, C., Delga, H., Caruana, A., Leveque, M., Bourrain, M., Ravard Helffer, K., Chol, B., Nguyen, T., Bessou-Touya, S. and Castex-Rizzi, N. (2016) Anti-inflammatory and immunomodulatory effects of Aquaphilus dolomiae extract on *in vitro* models. *Clin. Cosmet. Investig. Dermatol.* **9**, 421-434.

Bao, L., Shi, V. Y. and Chan, L. S. (2012) IL-4 regulates chemokine CCL26 in keratinocytes through the Jak1, 2/Stat6 signal transduction pathway: Implication for atopic dermatitis. *Mol. Immunol.* **50**, 91-97.

Bao, L., Zhang, H. and Chan, L. S. (2013) The involvement of the JAK-STAT signaling pathway in chronic inflammatory skin disease atopic dermatitis. *JAKSTAT* **2**, e24137.

Boos, A. C., Hagl, B., Schlesinger, A., Halm, B. E., Ballenberger, N., Pinarci, M., Heinz, V., Kreilinger, D., Spielberger, B. D., Schimke-Marques, L. F., Sawalle-Belohradsky, J., Belohradsky, B. H., Przybilla, B., Schaub, B., Wollenberg, A. and Renner, E. D. (2014)

Atopic dermatitis, STAT3- and DOCK8-hyper-IgE syndromes differ in IgE-based sensitization pattern. *Allergy* **69**, 943-953.

Cha, H. Y., Ahn, S. H., Cheon, J. H., Park, I. S., Kim, J. T. and Kim, K. (2016) Hataedock treatment has preventive therapeutic effects in atopic dermatitis-induced nc/nga mice under high-fat diet conditions. *Evid. Based Complement. Alternat. Med.* **2016**, 1739760.

Chang, W. A., Hung, J. Y., Jian, S. F., Lin, Y. S., Wu, C. Y., Hsu, Y. L. and Kuo, P. L. (2016) Laricitrin ameliorates lung cancer-mediated dendritic cell suppression by inhibiting signal transducer and activator of transcription 3. *Oncotarget* **7**, 85220-85234.

Choi, E. J., Debnath, T., Tang, Y., Ryu, Y. B., Moon, S. H. and Kim, E. K. (2016) Topical application of Moringa oleifera leaf extract ameliorates experimentally induced atopic dermatitis by the regulation of Th1/Th2/Th17 balance. *Biomed. Pharmacother.* **84**, 870-877.

Drennan, S., D'Avola, A., Gao, Y., Weigel, C., Chrysostomou, E., Steele, A. J., Zenz, T., Plass, C., Johnson, P. W., Williams, A. P., Packham, G., Stevenson, F. K., Oakes, C. C. and Forconi, F. (2017) IL-10 production by CLL cells is enhanced in the anergic IGHV mutated subset and associates with reduced DNA methylation of the IL10 locus. *Leukemia* **31**, 1686-1694.

Fridman, J. S., Scherle, P. A., Collins, R., Burn, T., Neilan, C. L., Hertel, D., Contel, N., Haley, P., Thomas, B., Shi, J., Collier, P., Rodgers, J. D., Shepard, S., Metcalf, B., Hollis, G., Newton, R. C., Yeleswaram, S., Friedman, S. M. and Vaddi, K. (2011) Preclinical evaluation of local JAK1 and JAK2 inhibition in cutaneous inflammation. *J. Invest. Dermatol.* **131**, 1838-1844.

He, Y., Sultana, I., Takeda, K. and Reed, J. L. (2017) Cutaneous deficiency of filaggrin and stat3 exacerbates vaccinia disease *in vivo*. *PLoS ONE* **12**, e0170070.

Holland, S. M., DeLeo, F. R., Elloumi, H. Z., Hsu, A. P., Uzel, G., Brodsky, N., Freeman, A. F., Demidowich, A., Davis, J., Turner, M. L., Anderson, V. L., Darnell, D. N., Welch, P. A., Kuhns, D. B., Frucht, D. M., Malech, H. L., Gallin, J. I., Kobayashi, S. D., Whitney, A. R., Voyich, J. M., Musser, J. M., Woellner, C., Schaffer, A. A., Puck, J. M. and Grimbacher, B. (2007) STAT3 mutations in the hyper-IgE syndrome. *N. Engl. J. Med.* **357**, 1608-1619.

Kang, G. J., Kang, N. J., Han, S. C., Koo, D. H., Kang, H. K., Yoo, B. S. and Yoo, E. S. (2012) The chloroform fraction of carpinus tschonoskii leaves inhibits the production of inflammatory mediators in HaCaT keratinocytes and RAW264.7 macrophages. *Toxicol. Res.* **28**, 255-262.

Kang, J. S., Lee, C. W., Lee, K., Han, M. H., Lee, H., Youm, J. K., Jeong, S. K., Park, B. D., Han, S. B., Han, G., Park, S. K. and Kim, H. M. (2008) Inhibition of skin inflammation and atopic dermatitis by topical application of a novel ceramide derivative, K112PC-5, in mice. *Arch. Pharm. Res.* **31**, 1004-1009.

Karuppagounder, V., Arumugam, S., Thandavarayan, R. A., Pitchaimani, V., Sreedhar, R., Afrin, R., Harima, M., Suzuki, H., Nomoto, M., Miyashita, S., Suzuki, K., Nakamura, M. and Watanabe, K. (2015) Modulation of HMGB1 translocation and RAGE/NFκB cascade by quercetin treatment mitigates atopic dermatitis in NC/Nga transgenic mice. *Exp. Dermatol.* **24**, 418-423.

Karuppagounder, V., Arumugam, S., Thandavarayan, R. A., Pitchaimani, V., Sreedhar, R., Afrin, R., Harima, M., Suzuki, H., Nomoto, M., Miyashita, S., Suzuki, K. and Watanabe, K. (2014) Resveratrol attenuates HMGB1 signaling and inflammation in house dust mite-induced atopic dermatitis in mice. *Int. Immunopharmacol.* **23**, 617-623.

Kim, D. C., Lee, H. S., Ko, W., Lee, D. S., Sohn, J. H., Yim, J. H., Kim, Y. C. and Oh, H. (2014) Anti-inflammatory effect of methylpenicinoline from a marine isolate of Penicillium sp. (SF-5995): inhibition of NF-κB and MAPK pathways in lipopolysaccharide-induced RAW264.7 macrophages and BV2 microglia. *Molecules* **19**, 18073-18089.

Kim, H. S., Park, S. Y., Kim, E. K., Ryu, E. Y., Kim, Y. H., Park, G. and Lee, S. J. (2012) Acanthopanax senticosus has a heme oxygenase-1 signaling-dependent effect on Porphyromonas gingivalis lipopolysaccharide-stimulated macrophages. *J. Ethnopharmacol.* **142**, 819-828.

Koppes, S. A., Brans, R., Ljubojevic Hadzavdic, S., Frings-Dresen, M. H., Rustemeyer, T. and Kezic, S. (2016) Stratum corneum tape stripping: monitoring of inflammatory mediators in atopic dermatitis patients using topical therapy. *Int. Arch. Allergy Immunol.* **170**, 187-193.

Kumari, S., Bonnet, M. C., Ulvmar, M. H., Wolk, K., Karagianni, N., Witte, E., Uthoff-Hachenberg, C., Renauld, J. C., Kollias, G., Toftgard, R., Sabat, R., Pasparakis, M. and Haase, I. (2013) Tumor necrosis factor receptor signaling in keratinocytes triggers interleukin-24-dependent psoriasis-like skin inflammation in mice. *Immunity* **39**, 899-911.

Lee, C. H., Hong, C. H., Yu, W. T., Chuang, H. Y., Huang, S. K., Chen, G. S., Yoshioka, T., Sakata, M., Liao, W. T., Ko, Y. C. and Yu, H. S. (2012) Mechanistic correlations between two itch biomarkers, cytokine interleukin-31 and neuropeptide β-endorphin, via STAT3/calcium axis in atopic dermatitis. *Br. J. Dermatol.* **167**, 794-803.

Lee, J. K., Lee, S., Baek, M. C., Lee, B. H., Lee, H. S., Kwon, T. K., Park, P. H., Shin, T. Y., Khang, D. and Kim, S. H. (2017) Association between perfluorooctanoic acid exposure and degranulation of mast cells in allergic inflammation. *J. Appl. Toxicol.* **37**, 554-562.

Lee, Y. J., Kim, J. E., Kwak, M. H., Go, J., Kim, D. S., Son, H. J. and Hwang, D. Y. (2014) Quantitative evaluation of the therapeutic effect of fermented soybean products containing a high concentration of GABA on phthalic anhydride-induced atopic dermatitis in IL-4/Luc/CNS-1 Tg mice. *Int. J. Mol. Med.* **33**, 1185-1194.

Lim, S. J., Kim, M., Randy, A., Nam, E. J. and Nho, C. W. (2016) Effects of Hovenia dulcis Thunb. extract and methyl vanillate on atopic dermatitis-like skin lesions and TNF-α/IFN-γ-induced chemokines production in HaCaT cells. *J. Pharm. Pharmacol.* **68**, 1465-1479.

Lyu, Y., Zhu, L., Qi, R., Xu, J., Di, Z., Chen, H. and Gao, X. (2014) Serum levels of suppressor of cytokine signaling 3 and signal transducer and activator of transcription 3 in childhood atopic dermatitis. *Chin. Med. J.* **127**, 2389-2391.

Matsuda, H., Watanabe, N., Geba, G. P., Sperl, J., Tsudzuki, M., Hiroi, J., Matsumoto, M., Ushio, H., Saito, S., Askenase, P. W. and Ra, C. (1997) Development of atopic dermatitis-like skin lesion with IgE hyperproduction in NC/Nga mice. *Int Immunol.* **9**, 461-466.

Mengoni, E. S., Vichera, G., Rigano, L. A., Rodriguez-Puebla, M. L., Galliano, S. R., Cafferata, E. E., Pivetta, O. H., Moreno, S. and Vojnov, A. A. (2011) Suppression of COX-2, IL-1β and TNF-α expression and leukocyte infiltration in inflamed skin by bioactive compounds from *Rosmarinus officinalis* L. *Fitoterapia* **82**, 414-421.

Oliveira Gde, A., de Oliveira, A. E., da Conceicao, E. C. and Leles, M. I. (2016) Multiresponse optimization of an extraction procedure of carnosol and rosmarinic and carnosic acids from rosemary. *Food Chem.* **211**, 465-473.

Orita, K., Hiramoto, K., Kobayashi, H., Ishii, M., Sekiyama, A. and Inoue, M. (2011) Inducible nitric oxide synthase (iNOS) and α-melanocyte-stimulating hormones of iNOS origin play important roles in the allergic reactions of atopic dermatitis in mice. *Exp. Dermatol.* **20**, 911-914.

Ortuno, J., Serrano, R. and Banon, S. (2015) Antioxidant and antimicrobial effects of dietary supplementation with rosemary diterpenes (carnosic acid and carnosol) vs vitamin E on lamb meat packed under protective atmosphere. *Meat Sci.* **110**, 62-69.

Park, K. W., Kundu, J., Chae, I. G., Kim, D. H., Yu, M. H., Kundu, J. K. and Chun, K. S. (2014) Carnosol induces apoptosis through generation of ROS and inactivation of STAT3 signaling in human colon cancer HCT116 cells. *Int. J. Oncol.* **44**, 1309-1315.

Riis, J. L., Vestergaard, C., Hjuler, K. F., Iversen, L., Jakobsen, L., Deleuran, M. S. and Olsen, M. (2016) Hospital-diagnosed atopic dermatitis and long-term risk of myocardial infarction: a population-based follow-up study. *BMJ Open* **6**, e011870.

Rocha, J., Eduardo-Figueira, M., Barateiro, A., Fernandes, A., Brites, D., Bronze, R., Duarte, C. M., Serra, A. T., Pinto, R., Freitas, M., Fernandes, E., Silva-Lima, B., Mota-Filipe, H. and Sepodes, B. (2015) Anti-inflammatory effect of rosmarinic acid and an extract of *Rosmarinus officinalis* in rat models of local and systemic inflammation. *Basic Clin. Pharmacol. Toxicol.* **116**, 398-413.

Sae-Wong, C., Mizutani, N., Kangsanant, S. and Yoshino, S. (2016) Topical skin treatment with Fab fragments of an allergen-specific IgG1 monoclonal antibody suppresses allergen-induced atopic dermatitis-like skin lesions in mice. *Eur. J. Pharmacol.* **779**, 131-137.

Sanchez, C., Horcajada, M. N., Membrez Scalfo, F., Ameye, L., Offord, E. and Henrotin, Y. (2015) Carnosol inhibits pro-inflammatory and

catabolic mediators of cartilage breakdown in human osteoarthritic chondrocytes and mediates cross-talk between subchondral bone osteoblasts and chondrocytes. *PLoS ONE* **10**, e0136118.

Schwager, J., Richard, N., Fowler, A., Seifert, N. and Raederstorff, D. (2016) Carnosol and related substances modulate chemokine and cytokine production in macrophages and chondrocytes. *Molecules* **21**, 465.

Shershakova, N., Baraboshkina, E., Andreev, S., Purgina, D., Struchkova, I., Kamyshnikov, O., Nikonova, A. and Khaitov, M. (2016) Anti-inflammatory effect of fullerene C60 in a mice model of atopic dermatitis. *J. Nanobiotechnology* **14**, 8.

Siegel, A. M., Stone, K. D., Cruse, G., Lawrence, M. G., Olivera, A., Jung, M. Y., Barber, J. S., Freeman, A. F., Holland, S. M., O'Brien, M., Jones, N., Nelson, C. G., Wisch, L. B., Kong, H. H., Desai, A., Farber, O., Gilfillan, A. M., Rivera, J. and Milner, J. D. (2013) Diminished allergic disease in patients with STAT3 mutations reveals a role for STAT3 signaling in mast cell degranulation. *J. Allergy Clin. Immunol.* **132**, 1388-1396.

Stempelj, M., Kedinger, M., Augenlicht, L. and Klampfer, L. (2007) Essential role of the JAK/STAT1 signaling pathway in the expression of inducible nitric-oxide synthase in intestinal epithelial cells and its regulation by butyrate. *J. Biol. Chem.* **282**, 9797-9804.

Sung, J. E., Kwak, M. H., Kim, J. E., Lee, Y. J., Kim, R. U., Kim, E. A., Lee, G. Y., Kim, D. S. and Hwang, D. Y. (2013) Therapeutic effects of fermented soycrud on phenotypes of atopic dermatitis induced by phthalic anhydride. *Lab. Anim. Res.* **29**, 103-112.

Sung, Y. Y., Lee, A. Y. and Kim, H. K. (2016) Forsythia suspensa fruit extracts and the constituent matairesinol confer anti-allergic effects in an allergic dermatitis mouse model. *J. Ethnopharmacol.* **187**, 49-56.

Suzuki, H., Makino, Y., Nagata, M., Furuta, J., Enomoto, H., Hirota, T., Tamari, M. and Noguchi, E. (2016) A rare variant in CYP27A1 and its association with atopic dermatitis with high serum total IgE. *Allergy* **71**, 1486-1489.

Szczepanik, A. M. and Ringheim, G. E. (2003) IL-10 and glucocorticoids inhibit Aβ(1-42)- and lipopolysaccharide-induced pro-inflammatory cytokine and chemokine induction in the central nervous system. *J. Alzheimers Dis.* **5**, 105-117.

Takeda, K., Clausen, B. E., Kaisho, T., Tsujimura, T., Terada, N., Forster, I. and Akira, S. (1999) Enhanced Th1 activity and development of chronic enterocolitis in mice devoid of Stat3 in macrophages and neutrophils. *Immunity* **10**, 39-49.

Tsunekawa, T., Banno, R., Mizoguchi, A., Sugiyama, M., Tominaga, T., Onoue, T., Hagiwara, D., Ito, Y., Iwama, S., Goto, M., Suga, H., Sugimura, Y. and Arima, H. (2017) Deficiency of PTP1B attenuates hypothalamic inflammation via activation of the JAK2-STAT3 pathway in microglia. *EBioMedicine* **16**, 172-183.

Tyagi, A., Agarwal, C., Dwyer-Nield, L. D., Singh, R. P., Malkinson, A. M. and Agarwal, R. (2012) Silibinin modulates TNF-α and IFN-γ mediated signaling to regulate COX2 and iNOS expression in tumorigenic mouse lung epithelial LM2 cells. *Mol. Carcinog.* **51**, 832-842.

Yao, H., Chen, Y., Zhang, L., He, X., He, X., Lian, L., Wu, X. and Lan, P. (2014) Carnosol inhibits cell adhesion molecules and chemokine expression by tumor necrosis factor-α in human umbilical vein endothelial cells through the nuclear factor-κB and mitogen-activated protein kinase pathways. *Mol. Med. Rep.* **9**, 476-480.

You, C. E., Moon, S. H., Lee, K. H., Kim, K. H., Park, C. W., Seo, S. J. and Cho, S. H. (2016) Effects of emollient containing bee venom on atopic dermatitis: a double-blinded, randomized, base-controlled, multicenter study of 136 patients. *Ann. Dermatol.* **28**, 593-599.

Zhang, L., Tao, L., Shi, T., Zhang, F., Sheng, X., Cao, Y., Zheng, S., Wang, A., Qian, W., Jiang, L. and Lu, Y. (2015) Paeonol inhibits B16F10 melanoma metastasis *in vitro* and *in vivo* via disrupting proinflammatory cytokines-mediated NF-κB and STAT3 pathways. *IUBMB Life* **67**, 778-788.